Acylation of Class A β-lactamases by Penicillins: A Theoretical Examination of the Role of Serine 130 and the β-lactam Carboxylate Group

Natalia Díaz,[†] Dimas Suárez,[‡,§] Tomás L. Sordo,[†] and Kenneth M. Merz, Jr.*[,‡]

Departamento de Química Física y Analítica, Universidad de Oviedo, C/Julián Clavería 8, 33006 Oviedo. Asturias. Spain, and Department of Chemistry, Eberly College of Sciences, The Pennsylvania State University, 152 Davey Laboratory, University Park, Pennsylvania 16802-6300

Received: July 26, 2001

Herein we present results of a computational study on the benzylpenicillin acylation of the class A TEM1 β-lactamase via hydroxyl-only and hydroxyl and carboxylate assisted processes. These mechanisms correspond to a one-step Ser130-assisted process and a second route in which the β-lactam carboxylate and the Ser130 hydroxyl group help the proton transfer from the hydroxyl group of Ser70 to the β-lactam leaving N atom. The internal geometry of the reactive part of the TEM1-benzylpenicillin system is taken from a B3LYP/6-31+G* computational study on the methanol-assisted methanolysis reaction of a penicillin model compound (3α-carboxypenam). The 6-acylamino side chain and the 2-methyl groups of benzylpenicillin, together with the closer residues around the essential Ser70, are relaxed by carrying out geometry optimizations with a hybrid QM/MM method. The corresponding relative energies in the protein combine the B3LYP/6-31+G* electronic energies of the reactive subsystem with semiempirical PM3 energies of the TEM1-benzylpenicillin systems both in vacuo and in solution. The PM3 calculations on the TEM1-benzylpenicillin systems are performed with a Divide and Conquer linear-scaling method. The hydroxyl and carboxylate assisted pathway, which is the most favored one, is in agreement with the experimentally observed kinetic isotope effects and is also compatible with the effects of mutagenesis experiments on the Ser130 residue. These results suggest that a similar mechanism for the formation of acylenzyme intermediates could be relevant to other active-site serine penicillin-recognizing enzymes.

Introduction

Bacterial resistance to β-lactam antibiotics has emerged over the past decades as a major health problem.[1−3] The most important mechanism through which bacteria have become resistant to β-lactam activity is the production of hydrolytic enzymes known as β-lactamases.[4−6] These enzymes can be chromosome or plasmid encoded and are secreted into the periplasmic space of Gram-negative bacteria or into the outer medium by Gram-positive bacteria. The most efficient therapeutic response against antimicrobial resistance, which is relentlessly fueled by natural selection, demands a continuous strategy of modification of known antibiotics, synthesis of new β-lactams and development of inhibitors of β-lactamases to be co-administered with normal β-lactam antibiotics. Therefore, understanding of the catalytic machinery of β-lactamases is crucial for the design of both β-lactamase inhibitors and new β-lactams with improved activity against bacteria.

All the β-lactam-recognizing enzymes in bacteria are proteases which differ mainly in their kinetic behavior and, to some extent, in their constitution.[7] In general, after establishing the corresponding Michaelis complex, β-lactams react toward β-lactam-recognizing enzymes via the formation of an acylenzyme intermediate. In a second step, the acylenzyme intermediate undergoes catalytic hydrolysis in order to regenerate the active site for the next turnover. Whether a β-lactam acylates and thereby inhibits the enzyme, or is finally hydrolyzed and inactivated, depends on the relative magnitudes of the kinetic constants for the acylation (k_{acyl}) and hydrolysis (k_{hyd}). Thus, the DD-peptidases that catalyze the peptidoglycan biosynthesis, generically termed Penicillin-Binding Proteins (PBPs), are inhibited by the formation of a stable β-lactam-enzyme intermediate ($k_{acyl} \gg k_{hyd}$) whereas β-lactamases subvert the antibiotic activity of β-lactams through a fast hydrolysis of the acylenzyme intermediates ($k_{acyl} \approx k_{hyd}$). This simple acylenzyme pathway has become the key mechanism that characterizes the action of PBPs and β-lactamases.[4−7]

The mechanistic division of β-lactamases is into the serine enzymes, in which the hydroxyl group of the essential serine acylates the β-lactam substrates, and into the zinc metalloenzymes, where the zinc ion(s) in the active site efficiently catalyze the hydrolysis of a broad spectrum of β-lactam antibiotics. For historical reasons,[4] the usual classification of these enzymes is based on the comparison of the amino acid sequences. This separates the serine β-lactamases into three classes A, C, and D, whereas the zinc-β-lactamases are grouped together into the structurally and kinetically heterogeneous class B. The zinc-β-lactamases have recently become a major research problem because antibiotic resistance mediated by these enzymes comprises an increasing challenge to the therapeutic future of β-lactam antibiotics.[8,9] However, the serine β-lactamases outnumber the zinc-enzymes and are considered a more immediate threat. Moreover, the serine β-lactamase inhibitors which are currently available, are not active against all class A and class

* To whom correspondence should be addressed. E-mail: merz@psu.edu. Fax: (814) 863 8403.
[†] Departamento de Química Física y Analítica, Universidad de Oviedo.
[‡] Department of Chemistry, Eberly College of Sciences, The Pennsylvania State University.
[§] On leave from Departamento Química Física y Analítica. Universidad de Oviedo.

10.1021/jp012881h CCC: $20.00
Published on Web 10/20/2001

C β-lactamases and there is a growing need for new broad-spectrum β-lactamase inhibitors.[2,3]

Among serine β-lactamases, the class A enzymes[10] constitute the majority of penicillin destroying enzymes and, therefore, have been intensively studied by means of high-resolution X-ray crystallography,[11−14] enzyme kinetics,[15,16] numerous site-directed mutagenesis experiments,[17−19] and molecular simulations.[20−31] On the basis of this large amount of data, the active-site residues which have been found to play an important catalytic role in the mechanism of all the class-A β-lactamases are the following: Ser70, Lys73, Lys234, Glu166, and Ser130, according to the sequence numbering of Ambler et al.,[32] and the water molecules Wat1−Wat3. However, the exact chemical roles of these active site residues and water molecules have not been resolved, except for the hydroxyl group of the nucleophilic Ser70. In addition, the side chains and/or backbone atoms of other residues (Asn170, Ala237, Arg244, etc.) stabilize the Michaelis complex and the acylenzyme intermediate. In particular, the main-chain N atoms of Ser70 and Ala237 form the so-called "oxyanion hole" which interacts with the oxygen of the β-lactam carbonyl group.[13]

General base catalysis is thought to increase the nucleophilicity of Ser70 although the identity of the residue that serves this function in the class-A β-lactamases remains an open question. For the acylation step of the reaction, a widely accepted hypothesis suggests that the conserved Glu166 residue is the general base which accepts a proton from Ser70 either directly or mediated by Wat1.[10,24] This proton could then be delivered to the leaving nitrogen atom through a network of hydrogen bonds involving Lys73, a second water molecule Wat2 and the hydroxyl group of Ser130. Alternatively, others have assumed that the ϵ-amino group of Lys73, which has a close contact with Ser70 in the crystal structure, remains neutral due to the active site environment.[13] Thus, Lys73 could act as a general base catalyzing the acylation step while the hydroxyl group of Ser130 could participate in the proton transfer to the β-lactam N atom.

For the hydrolysis of the acylenzyme, there is a consensus that Glu166 activates Wat1 for attack on the carbonyl carbon. This also ensures that a proton is available to protonate the Oγ atom of Ser70 after the re-entry of a water molecule.[10] This mechanistic proposal for deacylation has found strong experimental support from data obtained with cefoxitin and other compounds, which have a methoxy group capable of displacing the Wat1 molecule. As indicated by this mechanistic proposal, compounds of this type have been found to impede the hydrolysis of the acylenzyme intermediate.[33]

Of particular interest for understanding the mechanism of class A β-lactamases are the pH profiles of the steady-state kinetic parameters which are approximately bell-shaped with rate controlling ionization constants p$K_{a,1}$, and p$K_{a,2}$, centered on values of ∼4.4 and ∼8.2, respectively.[10] Experimentally, it has been concluded that Glu166 is the only residue that can account for p$K_{a,1}$ whereas p$K_{a,2}$ reflects the ionization state of Lys234.[10,19] Continuum electrostatic calculations[34,35] for several β-lactamases in the absence and presence of different types of β-lactam antibiotics have assigned the pK_a for Lys73 above 10, which is in agreement with experimental pK_a determinations.[36] It has been observed that, in both the substrate-free and the substrate-complexed forms of class A β-lactamases, only one residue adopts a non standard protonation state at neutral pH: Asp214.[34,35] These results are clearly inconsistent with the mechanistic proposals which assume that an initially unprotonated Lys73 could act as the general base. However, the acylation mechanism assisted by Glu166 seems structurally disfavored because of the relatively large distance separating the Ser70 and Glu166 side chains.[13] Moreover, site-directed mutagenesis experiments performed on Glu166 have also failed to supply a definitive picture for its role in acylation.[17] Moreover, kinetic isotope effects have revealed that enzyme deacylation may be a classic general-base-catalyzed hydrolysis but that there is little proton motion in the enzyme acylation transition state. This suggests a mechanism involving asymmetric double-displacement using different functional groups for acylation and deacylation.[16]

Several molecular modeling studies have attempted to elucidate the mechanistic pathway for the acylation of class A β-lactamases. For example, it has been proposed that the carboxylate group of the substrate could activate the Ser130 hydroxyl group and then the oxyanion of Ser130 would deprotonate the ammonium group of Lys73, which in turn would act as the general base for activation of the essential Ser70 residue.[23] A more complex reaction pathway, based on estimates of the electrostatic contributions to the free energy changes accompanying the conversion of the free enzyme into the acylenzyme intermediate, has been proposed.[31] Specifically, these electrostatic calculations indicated that the acid-catalyzed protonation of the β-lactam nitrogen through the β-lactam carboxylate group, the Ser130 and Lys234 side chains and a water molecule, would trigger the nucleophilic attack of Ser70 with proton abstraction catalyzed by the Wat1 molecule interacting with Glu166. A simpler mechanism has been studied by means of quantum chemical calculations on model systems followed by rigid docking of transition structures into the active site of the class A TEM1 β-lactamase.[25] In this study, the authors have argued that a one-step mechanism for acylation involving the nucleophilic serine Ser70 and the Ser130 hydroxyl group in class A enzymes might be a viable alternative. This latter mechanism would be the same for classes A and C of serine β-lactamases, but the Ser130 residue would be replaced by Tyr150 in the class C enzymes. A similar mechanism has been proposed for the mode of action of PBPs in which the alcoholysis reaction between the active site serine and the β-lactam substrate would proceed through a water-assisted concerted mechanism.[7,37]

In the present work, we explore the viability of hydroxyl-assisted pathways for the acylation step of class A β-lactamases through the use of quantum chemical and molecular modeling methodologies. Two mechanisms were considered (see Scheme 1): (a) a Ser70 nucleophilic attack with simultaneous fission of the β-lactam ring and proton transfer to the leaving N atom assisted by the hydroxyl group of Ser130. This mechanism coincides with the mechanisms previously studied in refs 25 and 37. (b) In the second mechanism, the Ser130 hydroxyl group mediates the proton transfer from the attacking nucleophilic group of Ser70 to the carboxylate group of the β-lactam substrate to form a tetrahedral species. The subsequent cleavage of the β-lactam ring proceeds with synchronous proton transfer from the carboxylic group to the endocyclic N atom of the β-lactam. This role for the carboxylate group resembles that observed in the hydrolysis reaction of aspirin where the carboxylate group acts as a general base catalyst.[38] We also note that a similar pathway has been described for the water-assisted methanolysis of penicillin compounds using semiempirical methods[7] and for the water-assisted aminolysis reaction of penicillins.[39]

We first investigate, at high levels of theory, the Potential Energy Surface (PES) for the neutral hydrolysis of a small system relative to the enzymatic substrates (**1** in Scheme 2).

SCHEME 1

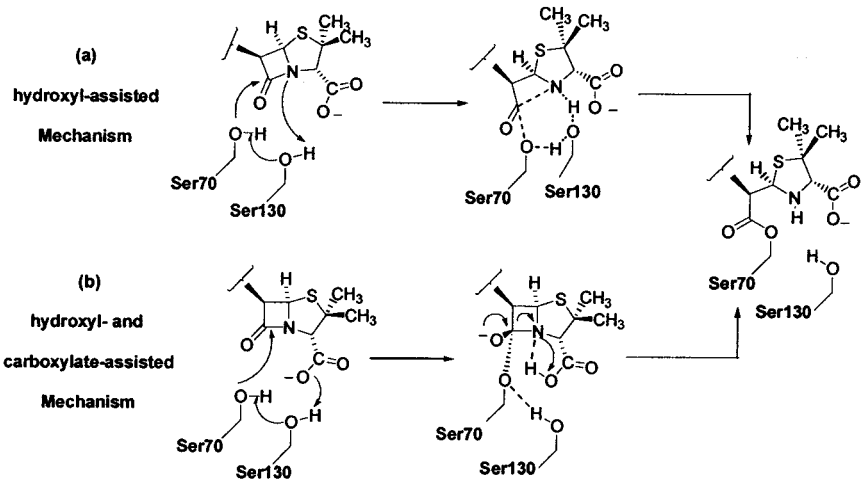

SCHEME 2

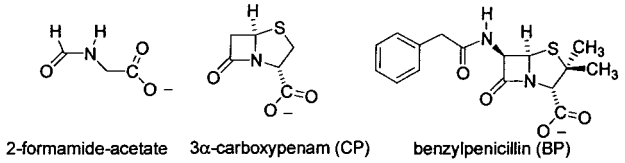

On the basis of these results, we calibrate the energetics and structures predicted by a Density Functional Theory (DFT) method. Second, the methanol-assisted methanolysis of a model penicillin compound (3α-carboxypenam, **2** in Scheme 2), is fully characterized at a DFT level of theory. The effect of bulk solvent on the energy profile of this reference system is taken into account by means of a continuum model. Finally, the most important structures involved in the methanolysis of **2** are employed in building the internal geometry of a benzylpenicillin (BP, **3**, in Scheme 2) substrate and the side chains of Ser70 and Ser130 embedded in the protein framework of a typical class A β-lactamase (the TEM1 enzyme). In the TEM1-BP structures, the substituents of the bicyclic nucleus of benzylpenicillin, the environmental water molecules, and some protein residues are relaxed via energy minimization using a combined quantum mechanical and a molecular mechanical (QM/MM) method. The relaxed structures are then used to compute quantum mechanically an energy profile in the TEM1 protein for both mechanisms. We employ a linear-scaling semiempirical method coupled with a continuum solvent model to account for environmental effects. These semiempirical energies are then combined with DFT energies for the reactive part of the system, which is not as accurately described by semiempirical methods. The viability of the hydroxyl-assisted pathways for the acylation of class A β-lactamases is analyzed in terms of the estimated energy profile in the enzyme. The ability of the hydroxyl and carboxylate-assisted mechanism to account for several experimental observations regarding β-lactamase catalysis is also discussed. These theoretical results provide us with further insights into the catalytic processes taking place in the active site of serine β-lactamases.

Methods

Quantum Chemical Calculations. Ab initio and DFT quantum chemical calculations were carried out with the Gaussian 98 system of programs.[40] The water-assisted hydrolysis of the prototype system (2-formamide-acetate **1**) was studied at the MP2/6-31+G* and B3LYP/6-31+G* levels[41,42] of theory via locating the transition structures (TSs) and intermediates involved in a concerted process and in a stepwise mechanism. Electronic energies for the MP2/6-31+G* optimized structures were recomputed using the G2(MP2,SVP) scheme[43] which approximates the QCISD(T)/6-311+G(3df,2p) level of theory in an additive fashion.

For the methanolysis reaction of the negatively charged 3α-carboxypenam assisted by a second methanol molecule, molecular geometry optimizations followed by analytical frequency calculations were performed at the HF/3-21G* and B3LYP/6-31+G* levels of theory. Although the preliminary HF/3-21G* results are not presented in this work, Intrinsic Reaction Coordinate (IRC) HF/3-21G* calculations[44] were carried out to confirm the reaction paths on the Potential Energy Surface (PES) connecting the different TSs, intermediates and products. $\Delta G_{\text{gas-phase}}$ values were obtained by combining the B3LYP/6-31+G* electronic energies and thermal corrections at the same level of theory. To take into account condensed-phase effects,[45] the electrostatic solvation free energies in aqueous solution were computed by means of B3LYP/6-31+G* Self-Consistent Reaction Field Poisson−Boltzmann (SCRF−PB) calculations on the gas-phase geometries. In these calculations the solute is represented by a set of atomic charges and the solvent as a layer of charges at the solute molecular surface.[46,47] Addition of the relative solvation free energies to the $\Delta G_{\text{gas-phase}}$ values gives the $\Delta G_{\text{solution}}$ values. Atomic charges were computed by carrying out Natural Population Analysis (NPA) and using the corresponding B3LYP/6-31+G* density matrices.[48]

Construction of the TEM1-BP Models. The class A β-lactamase enzymes are medium-sized monomeric proteins which are made up of two structural domains (an all-α and an α/β domain).[10] The active site is situated in a groove between the two domains and is readily accessible to solvent. The catalytically important residues are located on one helix-turn (Ser70 and Lys73), on a short loop in the all α-domain (Ser130), on the innermost strand of a β-sheet (Lys234, Ala237) and on the Ω-loop (Glu166, Asn170). The active site environment is a mix of solvent and a structurally heterogeneous protein framework, which contains numerous polar and charged residues. As noted in previous work,[26] the chemistry of this active site is, to say the least, difficult to model computationally.

Herein, we develop a computational protocol to reproduce the *enthalpic* effects of the protein while the effect of bulk solvent is handled through a solvent continuum model. Thus,

we built a TEM1-BP model in which the protein environment is partially adapted to stabilize an intermediate configuration between the prereactive Michaelis complex and the acylenzyme intermediate (see below). This protein environment is held fixed during the docking of the B3LYP/6-31+G* critical structures involved in the reaction of 3α-carboxypenam (these critical structures were augmented with the side chains of benzylpenicillin). In this way, we assured that the computed relative energy differences in the protein would reflect the inherent stability of the reactive part and its interaction with the surrounding environment. We note, however, that a significant structural relaxation of the protein once the acylenzyme intermediate is formed, has been characterized by experimental data[49] and molecular dynamics simulations.[22] In agreement with these findings, the construction of our model for the TEM1-BP acylenzyme intermediate required the relaxation of the loops and turns within the active site region in order to properly accommodate the degraded form of the BP substrate. As a consequence, we found that the computed energy in the protein for the acylenzyme structure was no longer comparable with those of the precursor structures and, therefore, we will only discuss the structural details regarding the acylenzyme model.

Starting coordinates for the protein atoms and the crystallographic water molecules were taken from the solid-state structure of the TEM1 β-lactamase at 1.8 Å resolution (PDB ID code: 1BTL).[50] In addition, water molecules were added around the Oγ@Ser70 atom within 15.0 Å using the LEaP program.[51] The protonation state for the ionizable residues were set to their normal ionization state at pH 7, except Asp214 which is neutral in the TEM1 active site.[34] Na^+ counterions were placed by LEaP 10 Å beyond the Oγ@Ser70 atom to neutralize the −6 charge of the TEM1 model. Following energy minimization, a 15 Å active zone centered on the Oγ@Ser70 atom was defined, and only residues with at least one heavy atom within this sphere as well as the cap water molecules restrained at a 15 Å boundary, were allowed to move during a Molecular Dynamics (MD) simulation using the parm96 version of the AMBER force field.[52] The time step was 1.0 fs, and the SHAKE algorithm was used to constrain the X−H bond lengths at their equilibrium values. A nonbond pairlist cutoff of 15.0 Å was used, and the nonbonded pairlist was updated every 25 time steps. The ROAR 2.0 program[53] was used, and the temperature was maintained at 300 K during the MD simulation using the Nosé-Hoover chain algorithm for temperature coupling.[54]

After 100 ps of simulation time, the last configuration was subjected to energy minimization. The structure of a tetrahedral intermediate formed via the nucleophilic attack of the Ser70 hydroxyl group on benzylpenicillin was built by molecular modeling within the active site. This TEM1-BP system was divided into a QM region comprising the BP substrate and the Ser70 and Ser130 residues (66 atoms), which was treated by the PM3 Hamiltonian,[55] and the rest of the protein atoms and water molecules were represented by the AMBER force field. This QM/MM partition[56,57] was applied in all of the subsequent PM3/AMBER calculations. The vdW parameters for the BP atoms were assigned the values of similar atom types in the AMBER force field. Four hydrogen link atoms were placed at the C and N backbone atoms of Ser70 and Ser130 to cap the exposed valence sites due to the bonds crossing the QM−MM boundary.[56] The model of the tetrahedral intermediate was then subjected to energy minimization in order to properly relax the protein−substrate contacts. Finally, the coordinates corresponding to the bicyclic nucleus and the carboxylate group of BP, and the side chains of Ser70 and Ser130 were deleted and the resultant structure was employed as a template to dock the B3LYP/6-31+G* critical structures involved in the reaction of 3α-carboxypenam.

After having docked the prereactive complex, the transition states and the tetrahedral intermediate structures, only the BP substrate, the Ser70, Ser130, Lys73, Lys234 residues, and the water molecules were relaxed by carrying out PM3/AMBER minimizations. For the concerted TS and the first TS of the stepwise mechanism, geometrical constraints were imposed on the bicylic skeleton and the carboxylate group of BP, and on the Cβ-OγH moieties of the active site serine groups to preserve their internal B3LYP/6-31+G* geometries during energy minimization. In the case of the tetrahedral intermediate and the TS for proton transfer and β-lactam cleavage, the Ser130 residue plays only a passive role and, therefore, its position was fully relaxed. In the case of the Michaelis complex, only those atoms in the bicyclic nucleus plus the carboxylate group of BP were geometrically constrained. An analogous protocol was used to dock the acylenzyme model except that all of the residues with at least one atom within 10 Å from the Oγ@Ser70 atom were also subjected to energy minimization.

PM3/AMBER geometry optimizations were carried without a nonbond cutoff using the Limited Memory BFGS minimizer[58] implemented in ROAR 2.0.[53] In the final optimized structures, the root-mean-square residual gradient was always less than 0.001 kcal/(mol Å).

Energy Calculations on the TEM1-BP Structures. We used a composite procedure in order to estimate the energy profile for the hydrolysis of BP in the TEM1 active site. The following energy terms were computed separately for each of the docked structures (prereactive complex, TSs and tetrahedral intermediate):

The coordinates of the BP substrate and those of the Ser70 and Ser130 side chains, were extracted from the structures embedded in the protein and augmented with the coordinates of two H-link atoms at the Cβ atoms (these subsystems will be referred as the *reactive* subsystems in the TEM1-BP structures). Single-point B3LYP/6-31+G* and standard PM3 calculations were carried out on the reactive subsystems to obtain their energies denoted as $E_{\text{B3LYP/6-31+G*}}$(reactive) and E_{PM3}(reactive), respectively.

Single-point PM3 calculations were performed on the TEM1-BP systems using the Divide and Conquer (D&C) approach[59,60] ($E_{\text{PM3/D\&C}}$(protein-BP) energies). In these D&C calculations, explicit solvent molecules were not considered except Wat1 and Wat3, which lie in a relatively buried position close to the active site residues. The resultant systems consisted of 4216 atoms.

Incorporation of solvent effects within a QM methodology was accomplished by means of single-point semiempirical calculations on the TEM1-BP systems using the D&C algorithm merged with the Poisson−Boltzmann equation.[61] The resultant $\Delta G_{\text{solvation}}$(protein-BP) energies incorporate long-range solute−solvent interactions and the statistical weight of different solvent configurations.

To estimate the relative energies of the critical structures with respect to the prereactive complex, the different energy terms were combined in the following manner

$$\Delta E_{\text{composite}} \approx \Delta E_{\text{B3LYP/6-31+G*}}(\text{reactive}) + [\Delta E_{\text{PM3D\&C}}(\text{protein-BP}) - \Delta E_{\text{PM3}}(\text{reactive})] + \Delta\Delta G_{\text{solvation}}(\text{protein-BP}) \quad (1)$$

where the second term in brackets is a semiempirical correction due to the effect of the protein environment in vacuo to the

relative energies of the reactive subsystem computed at the higher level of theory. To compare the protein effects predicted by the linear-scaling D&C PM3 method with those obtained with the QM/MM hybrid approach, we also computed the PM3 heat of formation of the reactive part embedded in the field created by the AMBER charges of the surrounding residues ($E_{PM3/AMBER}$(protein-BP) energies).

We note that the inclusion of link atoms in the computation of the E_{PM3}(reactive) and $E_{B3LYP/6-31+G*}$(reactive) energies, should have only a minor influence. For example, we observed that the quantum link atom charges were essentially constant in the different structures suggesting that a minimal artifact would result from the presence of these virtual H atoms. Similarly, we found that the influence on the relative energies of switching between the PM3 and B3LYP/6-31+G* internal geometries of the hydroxyl group of Ser70 and Ser130, was minimal (less than 1 kcal/mol).

The DivCon99 program[62] was employed to perform the D&C and D&C−PB PM3 calculations using the dual buffer layer scheme (inner buffer layer of 4.0 Å and an outer buffer layer of 2.0 Å) with one protein residue per core. This D&C *subsetting* with a total buffer region of 6.0 Å gives generally accurate energies.[63] A cutoff of 9.0 Å was used for the off-diagonal elements of the Fock, 1-electron and density matrices. The D&C−PB calculations were carried out using the computational protocol described in detail elsewhere.[61]

Results and Discussion

First, we present results corresponding to the water-assisted hydrolysis of the model system 2-formamide-acetate, then those for the methanol-assisted methanolysis of the 3α-carboxypenam anion and, finally, we discuss the hydrolysis of benzylpenicillin in the active site of the TEM1 β-lactamase.

Water-Assisted Hydrolysis of 2-Formamide-acetate. To further asses the suitability of the B3LYP/6-31+G* methodology to study the hydrolysis of β-lactams, the water-assisted hydrolysis of an amidic bond in the negatively charged model system **1** was investigated. This model system has a carboxylate group and the same connectivity as the corresponding moiety in penicillin antibiotics. The previously described hydroxyl only and hydroxyl and carboxylate-assisted pathways were characterized on the PES (these mechanisms are very similar to those thoroughly discussed below for the hydrolysis of the 3α-carboxypenam anion). The results are summarized in Figure 1.

In general, both correlated methods (MP2/6-31+G* and B3LYP/6-31+G*) provide similar geometries for the TSs and intermediates located along the reaction coordinate. At the TS for the concerted mechanism (**TS_C-test**), the water-assisted proton transfer to the leaving amino group is nearly complete, whereas the rupture of the C−N bond and the formation of the C−O bond are in their initial stages. The calculated energy barriers with respect to separated reactants were 18.4 and 15.5 kcal/mol in terms of G2 and B3LYP/6-31+G* electronic energies, respectively. In the hydroxyl and carboxylate-assisted mechanism, the attacking water molecule in **TS_1-test** has already released one proton to the carboxylate group mediated by the ancillary water molecule. After the C−O bond is formed leading to a tetrahedral intermediate species, the carboxylic group transfers a proton to the N atom, facilitating the complete C−N bond cleavage via a stretching motion (see the series of structures **I_1-test**, **I_2-test**, **TS_2-test**, **I_3-test** and **TS_3-test** in Figure 1). Interestingly, all of the structures involved in the proton transfer to the leaving N atom are close in energy so that the **I_1-test**, **I_2-test**, and **I_3-test** species are predicted to be short-lived.

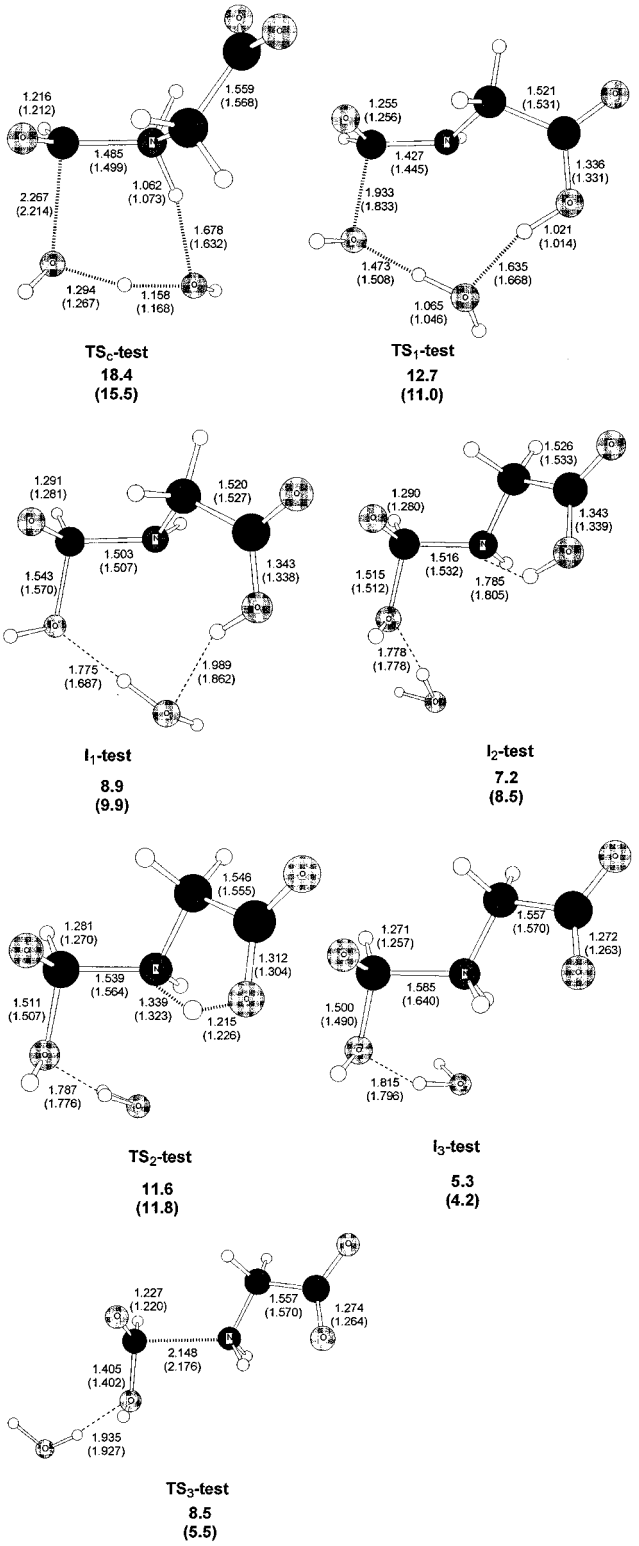

Figure 1. Optimized structures for the water-assisted and water and carboxylate-assisted hydrolysis of 2-formamide acetate. MP2/6-31+G* and (B3LYP/6-31+G*) distances in Å. G2(MP2,SVP) and (B3LYP/6-31+G*) relative energies with respect to separate reactants are also shown.

The G2(MP2,SVP) approach predicts that **TS_1-test** is the rate-determining transition state with an energy barrier of 12.7 kcal/mol (11.0 at the B3LYP/6-31+G* level) while the least stable structure at the B3LYP/6-31+G* level is the TS for protonation of the N atom, **TS_2-test**, with an energy barrier of 11.8 kcal/mol (11.6 at G2(MP2,SVP)). The G2(MP2,SVP) and the B3LYP/6-31+G* levels coincide in predicting the hydroxyl and

carboxylate-assisted pathway as the most favored mechanism in the gas-phase by around 5.5 and 2.5 kcal/mol, respectively. Overall, we conclude that B3LYP/6-31+G* is a reasonable level of theory to study the water-assisted hydrolysis of β-lactams although the stability of the hydroxyl-assisted concerted route could be moderately overestimated at this level.

Methanol-Assisted Methanolysis of 3α-Carboxypenam. To understand the molecular details of the combined role played by Ser70 and Ser130 in the class A β-lactamases, we studied the reaction between the 3α-carboxypenam anion and the dimer of methanol. The geometries for the critical structures located on the B3LYP/6-31+G* PES are shown in Figure 2 whereas their corresponding relative electronic energies and Gibbs energies both in the gas-phase and in solution are given in Table 1. Because the conversion of enzyme−substrate complexes to intermediates or transition states are unimolecular processes, the relative magnitudes in Table 1 are given with respect to the prereactive complex formed between carboxypenam and the methanol dimer.

The hydroxyl- and hydroxyl and carboxylate-assisted reaction pathways for the methanolysis of 3α-carboxypenam start from the same prereactive complex. In this complex, the catalytic methanol molecule bridges between the nucleophilic methanol and the β-lactam carboxylate group through short O−H···O H-bond contacts of 1.637 and 1.759 Å (see **C** in Figure 2). In addition, the orientation of the nucleophilic fragment is determined by a weak C−H···O interaction with a CH_2 group of the four-membered ring. The internal geometry of the β-lactam in **C** is weakly altered (e.g., the C−N amide and C−O carbonyl bonds are 1.378 and 1.219 Å, respectively, in the isolated reactant, but are 1.388 and 1.217 Å in **C**). In the methanol dimer, the distance between the C atoms (4.369 Å) is not far from that separating the Ser70 and Ser130 Cβ atoms in the solid-state structure (∼4.8 Å).[50] In terms of the electronic energy including ZPVE corrections, **C** is 24.8 kcal/mol more stable than the reactants ($\Delta G_{\text{gas-phase}} = -6.6$ kcal/mol).

The concerted hydroxyl-assisted mechanism proceeds through $\mathbf{TS_C}$ in which the auxiliary hydroxyl group catalyzes the proton transfer from the nucleophile to the N atom in the β-lactam ring (see Figure 2). The covalent bond formation at $\mathbf{TS_C}$ is early because the forming C−O bond is quite long (2.262 Å) and the endocyclic C−N bond is barely cleaved (1.546 Å). In contrast, proton transfer is much more advanced: the β-lactam N atom is nearly protonated at $\mathbf{TS_C}$ (N−H = 1.157 Å), whereas the H atom released by the nucleophile is at an intermediate position between both methanol molecules (O···H···O contacts of 1.251 and 1.161 Å). In agreement with the calculated geometry, the transition vector of $\mathbf{TS_C}$ is dominated by the motion of the reactive H atoms showing an imaginary frequency of 911 cm^{-1}. According to the NPA population analysis, the methanol dimer at $\mathbf{TS_C}$ develops a negative charge (∼ −0.6 e) which is delocalized throughout the O···H···O contact, whereas the carboxypenam fragment has a *zwitterionic* character. The $\Delta E_{\text{B3LYP/6-31+G*}}$ and $\Delta G_{\text{gas-phase}}$ values for $\mathbf{TS_C}$ with respect to the initial complex are 37.2 and 42.1 kcal/mol, respectively.

$\mathbf{TS_C}$ is connected with the product complex $\mathbf{P_C}$ shown in Figure 2 in which the catalytic methanol molecule hydrogen bonds with the ester group. With respect to the prereactive complex, $\mathbf{P_C}$ is less stable by 1.9 ($\Delta E_{\text{B3LYP/6-31+G*}}$) and 3.2 kcal/mol ($\Delta G_{\text{gas-phase}}$).

The H-bond network present in the prereactive complex is appropriate for the participation of the carboxylate group in the hydrogen shuttling required to form and, subsequently, cleave a tetrahedral intermediate. This is confirmed by the location of $\mathbf{TS_1}$ for the nucleopilic attack of methanol with methanol-assisted proton transfer to the carboxylate group (see Figure 2). Both the C−O bond formation and the proton-transfer events are more advanced in $\mathbf{TS_1}$ than in $\mathbf{TS_C}$. The forming C−O and O−H bonds at $\mathbf{TS_1}$ have equilibrium distances of 2.060 Å and 1.066, 1.025 Å, respectively. Moreover, the catalytic methanol molecule at $\mathbf{TS_1}$ bridges the carboxylic and methoxy groups via short H-bond contacts of 1.609 and 1.437 Å. Inspection of the NPA atomic charges confirm that the nucleophilic methanol molecule has an anionic character, because it has localized a negative charge of ∼ −0.8 e on its O atom. The transition vector of $\mathbf{TS_1}$ is dominated by the stretching motion for the formation of the C−O bond while the curvature of the energy profile in the neighborhood of $\mathbf{TS_1}$ is relatively flat ($\nu_{TS} = 158$ i cm^{-1}). In the gas-phase, $\mathbf{TS_1}$ is about 14 kcal/mol more stable than $\mathbf{TS_C}$ so that the energy barrier for $\mathbf{TS_1}$ is moderate, 22.9 kcal/mol ($\Delta E_{\text{B3LYP/6-31+G*}}$) and 27.5 kcal/mol ($\Delta G_{\text{gas-phase}}$).

$\mathbf{TS_1}$ is connected to a tetrahedral intermediate $\mathbf{I_1}$ which is only 0.7 kcal/mol more stable on the B3LYP/6-31+G* PES. Structurally, the equilibrium distance of the forming C−O bond is the main difference between these two critical points (1.557 Å at $\mathbf{I_1}$ vs 2.060 Å at $\mathbf{TS_1}$), whereas the bridging position of the catalytic methanol molecule is quite similar in both structures. The endocyclic C−N bond at $\mathbf{I_1}$ (1.558) is only 0.10 Å longer than at $\mathbf{TS_1}$. The global negative charge of $\mathbf{I_1}$ is concentrated on the carbonyl-like O atom and the β-lactam N atom with −0.82 e and −0.60 e NPA charges, respectively.

The rupture of the O···H−O···H−O bridge connecting the carboxylic and the nucleophilic O atom at $\mathbf{I_1}$ is required to form the final acyl species via protonation of the N atom. Figure 2 gives the structure of a second tetrahedral intermediate ($\mathbf{I_2}$) in which the β-lactam N atom has an intramolecular H-bond with the carboxylic group (OH···N 1.783 Å). Other structural features of this species places the second methanol molecule below the β-lactam ring where it solvates the exocyclic methoxy group via an H-bond of 1.792 Å, and the forming ester group adopts a nearly planar trans configuration. Several pathways, not detailed here, connect $\mathbf{I_1}$ and $\mathbf{I_2}$ via low barrier internal rotations. $\mathbf{I_2}$ is effectively a more advanced structure in terms of the lengthening (+0.11 Å) of the breaking C−N bond with respect to $\mathbf{I_1}$. $\mathbf{I_2}$ has $\Delta E_{\text{B3LYP/6-31+G*}}$ and $\Delta G_{\text{gas-phase}}$ values of 21.5 and 24.6 kcal/mol, respectively.

The $\mathbf{I_2}$ intermediate passes through a TS ($\mathbf{TS_2}$ in Figure 2) which is only 0.3 kcal/mol above it in terms of $\Delta G_{\text{gas-phase}}$. At $\mathbf{TS_2}$, the endocyclic C−N bond is clearly broken (1.984 Å), whereas the H shift from the carboxylic group to the forming amino group is in its initial stage. Thus, the fission of the amide bond in the bicyclic 3α-carboxypenam precedes the protonation of the leaving amino group. $\mathbf{TS_2}$ is 2.6 kcal/mol more stable than $\mathbf{TS_1}$ in terms of $\Delta G_{\text{gas-phase}}$ values. Thus, $\mathbf{TS_1}$ is the rate-determining TS for the hydroxyl and carboxylate-assisted process. $\mathbf{TS_2}$ is directly linked to the product complex $\mathbf{P_2}$ in Figure 2 which is about 5 kcal/mol more stable than that observed for the concerted route. $\mathbf{P_2}$ and $\mathbf{P_C}$ mainly differ in the ring-puckering of the five-membered ring, and the more stable conformer ($\mathbf{P_2}$) has the exocyclic carboxylate in an equatorial relationship.

Because the critical structures involved in the hydroxyl and carboxylate-assisted route are very close in energy on the B3LYP/6-31+G* PES, we emphasize that the existence of the tetrahedral intermediates in the gas-phase would at best transient. Moreover, some of the structures could appear or disappear at other levels of theory. Nevertheless, the series of structures $\mathbf{C \rightarrow [TS_1]^{\ddagger} \rightarrow I_1 \rightarrow I_2 \rightarrow [TS_2]^{\ddagger} \rightarrow P_2}$ give interesting mechanistic

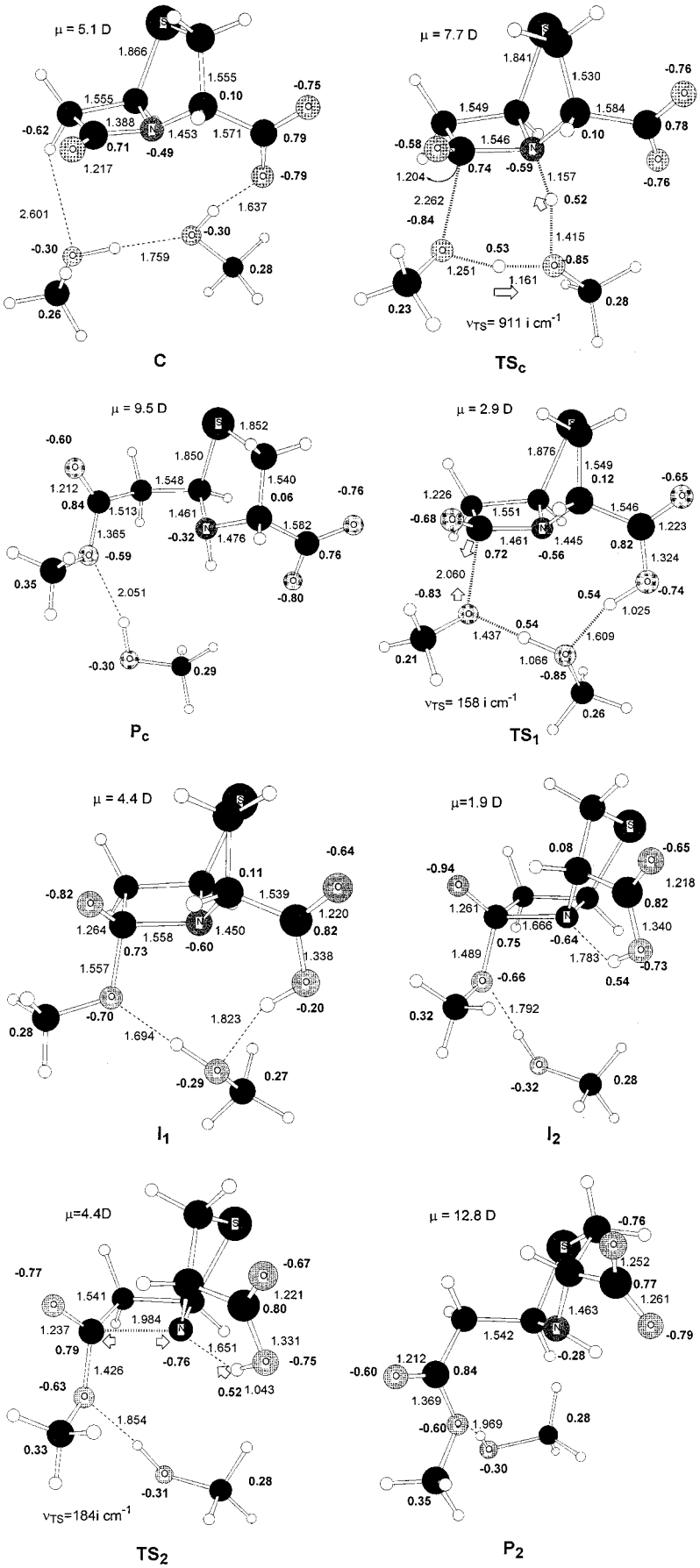

Figure 2. B3LYP/6-31+G* optimized structures for the methanol-assisted methanolysis reaction of 3α-carboxypenam. Distances in Å. B3LYP/6-31+G* NPA atomic charges in bold characters. Dipole moments (in Debyes) and frequencies corresponding to the transition vectors are also displayed. Transition vectors are also given.

TABLE 1: Relatives Energies (kcal/mol) of the Methanolysis Reaction of 3α-carboxypenam Assisted by a Second Molecule of Methanol

structures	B3LYP/6-31+G* [a]	$\Delta G_{\text{gas-phase}}$ [b]	$\Delta\Delta G_{\text{solvation}}$ [c]	$\Delta G_{\text{solution}}$ [d]
C	0.0 (0.0)	0.0	0.0 (0.0)	0.0
$\mathbf{TS_C}$	37.2 (41.4)	42.1	−5.5 (−3.9)	36.6
$\mathbf{P_C}$	1.9 (0.6)	3.2	−9.6 (−6.2)	−7.7
$\mathbf{TS_1}$	22.9 (24.7)	27.5	9.5 (7.2)	37.0
$\mathbf{I_1}$	22.2 (21.7)	26.4	4.9 (5.2)	31.3
$\mathbf{I_2}$	21.5 (21.2)	24.6	9.0 (7.2)	33.6
$\mathbf{TS_2}$	21.6 (22.2)	24.9	4.9 (8.7)	29.8
$\mathbf{P_2}$	−3.5 (−4.8)	−2.9	−11.8 (−7.9)	−14.7

[a] Including ZPVE correction from B3LYP/6-31+G* frequencies. Values in parentheses are pure electronic energies. [b] Using B3LYP/6-31+G* electronic energies and thermal corrections. [c] Relative values of the Electrostatic Solvation energies with respect to the pre-reactive complex from single-point B3LYP/6-31+G* SCRF−PB calculations. Values in parentheses were obtained from PM3 SCRF−PB calculations on the B3LYP/6-31+G* geometries. [d] From the B3LYP/6-31+G* $\Delta G_{\text{gas-phase}}$ and $\Delta\Delta G_{\text{solvation}}$ energies.

details regarding the ring-opening of the β-lactam ring via the hydroxyl and carboxylate-assisted hydrolysis. This process is predicted to occur in four consecutive stages: first the nucleophile transfers a proton to the carboxylate group with assistance from the catalytic hydroxyl group; second, the negatively charged nucleophile attacks the carbonyl group leading to a tetrahedral species. This second stage destabilizes the β-lactam ring and places a negative charge on the N atom which becomes subsequently stabilized by its interaction with the carboxylic group. In a third stage, the C−N amide bond is broken via a stretching motion. Finally, the leaving amino group accepts a proton from the carboxylic moiety. It should be noted that the energy barrier is determined by the C−O bond forming and C−N bond breaking events.

In light of the nature of the mechanisms found in the gas-phase, environment effects could have a considerable influence on this process. To address this important point, we first estimated the relative solvation energies in aqueous solution for all the critical structures ($\Delta\Delta G_{\text{solvation}}$ in Table 1) with respect to **C** by means of B3LYP/6-31+G* SCRF−PB calculations using the gas-phase geometries. For comparative purposes, we also included in Table 1 the $\Delta\Delta G_{\text{solvation}}$ values calculated at the PM3 level using a similar SCRF−PB approach. In solution, $\mathbf{TS_C}$ is electrostatically stabilized owing to its greater polarity. However, the global negative charge in each of the critical structures constituting the hydroxyl and carboxylate-assisted reaction coordinate are more delocalized, thereby decreasing the polarization of the solvent continuum (see dipole moments in Figure 2). As a consequence, the hydroxyl-assisted concerted mechanism with a $\Delta G_{\text{solution}}$ barrier of 36.6 kcal/mol, is slightly favored with respect to the hydroxyl and carboxylate-assisted route which has a $\Delta G_{\text{solution}}$ barrier of 37.0 kcal/mol corresponding to $\mathbf{TS_1}$. The continuum model also predicts that the energy differences among the structures involved in the hydroxyl and carboyxlate-assisted process can be substantially increased in solution, $\mathbf{TS_2}$ being 7.2 kcal/mol more stable than $\mathbf{TS_1}$.

The SCRF−PB results suggest that the effect of environment can play an important kinetic role on this mechanism and, therefore, the estimation of protein−substrate interactions and solvent effects along the reaction coordinate is necessary in order to assess the enzymatic feasibility of this class of mechanisms. In addition, comparison between the semiempirical $\Delta\Delta G_{\text{solvation}}$ values in Table 1 and the B3LYP/6-31+G* ones gives a measure of the quality of the environmental effects as estimated semiempirically. We see that the PM3 and B3LYP/6-31+G* $\Delta\Delta G_{\text{solvation}}$ terms predict an identical trend (i.e., $\mathbf{TS_C}$ becomes preferentially stabilized in solution). However, a significant numerical discrepancy occurs at $\mathbf{TS_2}$ where the PM3 computed $\Delta\Delta G_{\text{solvation}}$ (8.7 kcal/mol) overestimates the destabilization of $\mathbf{TS_2}$ in solution.

SCHEME 3

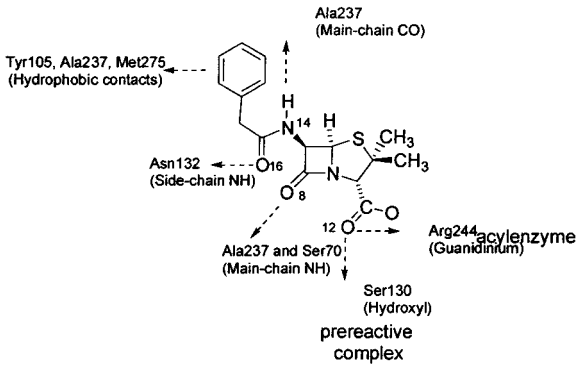

Hydrolysis of Benzylpenicillin in the Active Site of TEM1 β-Lactamase. To estimate the stability of the hydroxyl-only and hydroxyl and carboxylate-assisted pathways for the acylation of the TEM1 β-lactamase by BP, several TEM1-BP structures were constructed. In these structures, the geometry of the reactive part (the β-lactam and thiazolidine rings of BP and the side chains of Ser70 and Ser130) was taken from the prereactive complex **C**, the transition states ($\mathbf{TS_C}$, $\mathbf{TS_1}$, and $\mathbf{TS_2}$), and the tetrahedral intermediate $\mathbf{I_2}$ for the methanolysis reaction of 3α-carboxypenam. As described in the Methods section, a PM3/AMBER tetrahedral intermediate was used as a template to build the TEM1-BP models in which the forming ester group has a trans relationship as in the carboxypenam structure $\mathbf{I_2}$. Analogously, the internal geometry of the $\mathbf{P_2}$ product complex in Figure 2 was used to build the TEM1-BP acylenzyme model.

In Table S1 in the Supporting Information, the most significant H-bond contacts among the active site residues and the BP substrate (see Scheme 3) are characterized in terms of distances between heavy atoms. Table 2 collects the different relative energies corresponding to the TEM1-BP structures except the acylenzyme intermediate. Figure 3 displays a stereoview of the prereactive complex.

Protein−Substrate Contacts. The main residue−residue and protein−water contacts are maintained in the TEM1-BP prereactive complex with respect to those in the TEM1 native form.[50] For example, the Wat1 molecule remains in its bridging position between the Ser70 hydroxyl and the Glu166 carboxylate groups, whereas the ammonium groups of Lys73 and Lys234 interact with the hydroxyl groups of Ser70 and Ser130, respectively. Moreover, the most important enzyme−substrate binding determinants are also similar to those observed in previous molecular modeling studies.[20,21] Thus, the 6-acylamino side chain of BP contributes to substrate binding through H-bond interactions (O16@BP···Nδ@Asn132 = 2.84 Å, N14@BP···O@Ala237 = 3.28 Å) and hydrophobic contacts which are well maintained in all of the TEM1-BP structures. The β-lactam carbonyl O8 atom forms a H-bond interaction with the backbone N atom of Ala237 (O8@BP···N@Ala237 = 3.04 Å). Recent experimental results[64] have suggested that an interaction between O8 and the guanidinium group of Arg244 could induce some strain/distortion in the BP substrate. However, this distance is computed to be 4.4 Å, which reduces the ability of this interaction to induce strain in BP. On the other hand, the β-lactam carbonyl atom (C7) is placed close to the nucleophilic Oγ atom of Ser70 (3.83 Å). In the prereactive TEM1-BP complex, the side chains of Ser70, Ser130, and the β-lactam

TABLE 2: Relative Energies (kcal/mol) of the Structures Involved in the Acylation Reaction of Benzylpenicillin as Evaluated in Vacuum or in the Protein Environment of the TEM1 β-lactamase (see text for details)

structure	$\Delta E_{B3LYP/6-31+G^*}$ (reactive)[a] A	ΔE_{PM3} (reactive) B	$\Delta E_{PM3/D\&C}$ (protein-BP)[b] C	$\Delta E_{PM3/D\&C} - \Delta E_{PM3}$[b] C − B	$\Delta\Delta G_{solvation}$ (protein-BP) D	$\Delta E_{composite}$[c]
TEM1-BP **C**	0.0	0.0	0.0 (0.0)	0.0 (0.0)	0.0	0.0
TEM1-BP $\mathbf{TS_C}$	46.0	74.9	70.5 (99.6)	−4.4 (24.7)	−3.0	38.6
TEM1-BP $\mathbf{TS_1}$	24.8	36.4	31.0 (13.4)	−5.4 (−23.0)	6.5	25.9
TEM1-BP **I**	20.4	4.7	−2.4 (−13.2)	−7.1 (−17.9)	9.5	22.8
TEM1-BP $\mathbf{TS_2}$	19.9	8.4	6.4 (−9.9)	−2.0 (−18.3)	10.0	27.9

[a] Electronic energies. [b] $\Delta E_{PM3/AMBER}$ values are in parentheses. [c] $\Delta E_{composite} = \Delta E_{B3LYP/6-31+G^*}$(reactive) + [$\Delta E_{PM3D\&C}$(protein-BP) − ΔE_{PM3}(reactive)] + $\Delta\Delta G_{solvation}$(protein-BP).

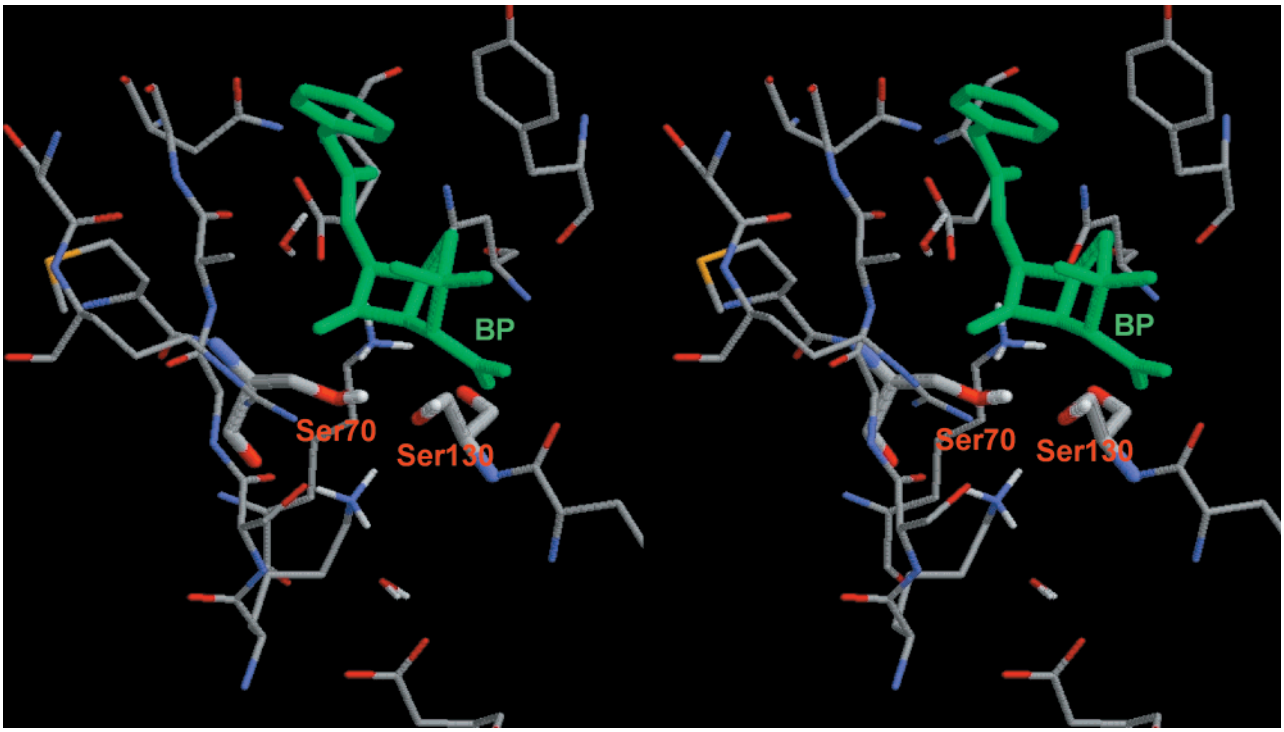

Figure 3. Stereoview of the PM3/AMBER minimized structure of the prereactive complex for the hydrolysis reaction of BP in the active site of the TEM1 β-lactamase.

carboxylate can be connected through a sequence of H-bonds (O−H···O−H···OCO) (see Figure 3). This simple H-bonding network defines the proton-transfer pathways required to give the $\mathbf{TS_C}$ or the $\mathbf{TS_1}$ configurations in the TEM1 active site.

On going from **C** to $\mathbf{TS_C}$ or to $\mathbf{TS_1}$ in the TEM1-BP models, the most remarkable change in protein−substrate interactions involves the strengthening of the Oγ@Ser130···Nζ@Lys73 and the Oγ@Ser130···Nζ@Lys234 contacts in $\mathbf{TS_C}$ and $\mathbf{TS_1}$, respectively. For the $\mathbf{TS_C}$ or $\mathbf{TS_1}$ configurations, the hydroxyl groups of Ser70 and Ser130 develop a negative charge which can be stabilized by salt bridge interactions with the ammonium groups of Lys73 and Lys234.

In view of the results obtained for the methanolysis of 3α-carboxypenam, we modeled a TEM1-BP tetrahedral configuration for the hydroxyl and carboxylate assisted pathway based on the $\mathbf{I_2}$ carboxypenam structure, whereas the cleavage of the β-lactam was represented by the $\mathbf{TS_2}$ carboxypenam structure embedded in the protein. The resultant **I** and $\mathbf{TS_2}$ TEM1-BP models show the hydroxyl group of Ser130 hydrogen bonding to the endocyclic N4 β-lactam atom (N4···Oγ@Ser130 ∼2.8 Å) which in turn interacts with the protonated carboxylate group. Most interestingly, the carbonylic O8 atom of BP at the **I** and $\mathbf{TS_2}$ configurations reinforces the H-bonds with the backbone N atom of Ala237 (O8@BP···N@Ala237 ∼2.8 Å) and the main-chain N atom of Ser70 (O8@BP···N@Ser70−3.3 Å), that is, the "oxyanion hole" groups. From these structural results, we see that the hydroxyl and carboxylate assisted mechanism shows favorable contacts all along the reaction coordinate.

From the $\mathbf{TS_2}$ TEM1-BP structure, shuttling the proton to the leaving N atom leads to the acylenzyme intermediate (also accessible from the $\mathbf{TS_C}$ TEM1-BP structure). In our model, the strength of the "oxyanion hole" contacts stabilizing the ester functionality of the acylenzyme intermediate is similar to that observed in the **I** and $\mathbf{TS_2}$ configurations. However, the partial relaxation of both the BP geometry and the protein surroundings introduces new protein−substrate contacts. In particular, the β-lactam carboxylate group has a salt bridge interaction with the guanidinium group of Arg244 (O12@BP···Nη2@Arg244 = 3.6 Å). Moreover, in the acylenzyme model, the Wat1 molecule, which forms an H-bond with the Glu166 carboxylate group, is favorably oriented to attack the C7 atom of the ester group (O···C7 = 2.89 Å) in agreement with the proposed catalytic role of Glu166 in the deacylation step.[10] Globally, the structural features of the acylenzyme model is in agreement with the X-ray determination of the acylenzyme structure trapped in the Glu166→Asn166 mutant of the TEM1 enzyme[13] and in that of the 6α-(hydroxymethyl) penicillinate inhibitor.[65]

Energy Profile. The different energetic components collected in Table 2 give us insights into the separate kinetic effects arising from the BP side chain ($\Delta E_{B3LYP/6-31+G^*}$ electronic energies, column **A** in Table 2), the protein−substrate interactions (ΔE_{PM3} and $\Delta E_{PM3/D\&C}$ energies, columns **B** and **C**), and solvent effects

($\Delta\Delta G_{Solvation}$, column **D**). For the concerted mechanism, the $\Delta E_{B3LYP/6\text{-}31+G^*}$ barrier corresponding to the reactive part in the TEM1-BP $\mathbf{TS_C}$ model, is 4.6 kcal/mol (41.4 (see Table 1) *vs* 46.0) higher than that for the unsubstituted 3α-carboxypenam. Most likely, this destabilization of the $\mathbf{TS_C}$ configuration is due to the fact that the penicillin amide group acquires a partial positive charge at $\mathbf{TS_C}$ which diminishes the inductive effect of the 6-acylamino side chain. On the other hand, the formation of the ester group at the **I** and $\mathbf{TS_2}$ configurations is slightly favored by the electronic effect of the 6-acylamino side by 0.8 and 2.3 kcal/mol, respectively.

Protein effects on the different model structures in the TEM1 active site are estimated semiempirically by energy differences computed as $\Delta E_{PM3/D\&C}$(protein-BP)-ΔE_{PM3}(reactive). According to these PM3 calculations, all of the TEM1-BP structures become stabilized. The concerted $\mathbf{TS_C}$ model is 4.4 kcal/mol more favorable in the protein while the $\mathbf{TS_1}$, **I** and $\mathbf{TS_2}$ configurations are stabilized by 5.4, 7.1, and 2.0 kcal/mol, respectively. The greatest stabilization was achieved by the tetrahedral configuration **I** in agreement with the strong "oxyanion hole" interactions between the negatively charged O8@BP atom and the main-chain NH group of Ala237. The salt bridge contacts between the OγSer70···H−Oγ@Ser130 anionic moiety and the adjacent ammonium groups of Lys73 and Lys234, probably contribute to the stabilization of the $\mathbf{TS_C}$ and $\mathbf{TS_1}$ TEM1-BP structures.

The relative solvation energies of the TEM1-BP models ($\Delta\Delta G_{solvation}$ in Table 2) reproduce the same trends observed for the carboxypenam model. Thus, the hydroxyl-only assisted route is electrostatically favored by solute−solvent interactions (−3.0 kcal/mol) and the hydroxyl and carboxylate-assisted pathway is disfavored by 6.5−10.0 kcal/mol. In particular, the cleavage of the β-lactam ring via the $\mathbf{TS_2}$ TEM1-BP structure turns out to be very disfavored by solvent effects (+10.0 kcal/mol) according to the PM3 D&C PB calculations.

By combining the different energy terms using the composite approach described in the Methods section, we provide an estimate of the enzymatic energy profile for both mechanisms. In the solvated protein, the acylation route assisted only by Ser130 has an energy barrier of 38.6 kcal/mol which is 10.7 kcal/mol higher than that computed for the $\mathbf{TS_2}$ TEM1-BP structure, which is the rate-determining step along the hydroxyl (Ser130) and carboxylate-assisted pathway. Therefore, these $\Delta E_{composite}$ values clearly show that the catalytic advantage of shuttling the Ser70 proton through both the Ser130 hydroxyl group and the penicillin carboxylate group, is preserved in the mixed protein−solvent environment. However, we note that the $\Delta E_{composite}$ barriers for the $\mathbf{TS_1}$ and $\mathbf{TS_2}$ configurations (∼26−28 kcal/mol), though moderate are not compatible with the fast kinetics exhibited by class-A β-lactamases. For example, the enzymatic hydrolysis of penicillins presents an acceleration of about 10^8 fold with respect to the alkaline hydrolysis reaction (the ΔG energy barrier for the alkaline hydrolysis of benzylpenicillin amounts to 19.0 kcal/mol at 30 °C).[5,66]

At this point, it is worthwhile to critically examine the accuracy of the protein and solvent effects predicted by the PM3 semiempirical calculations on the TEM1-BP structures. Importantly, the predicted changes in the protein−substrate interactions along the reaction profile are dependent on the QM or QM/MM methodology used. This is well-illustrated by the PM3/AMBER results also included in Table 2. In this case, the electrostatic interaction between a *hard* set of AMBER point charges representing the MM region and a *soft* PM3 charge density yields a catalytic effect for the hydroxyl and carboxylate-assisted pathway of ∼−20 kcal/mol. However, for the $\mathbf{TS_C}$ TEM1-BP model an anticatalytic effect of ∼+25 kcal/mol is observed. On the other hand, the PM3 D&C calculations take into account polarization and charge-transfer effects, thereby giving a more balanced description of the protein−substrate interactions in all of the TEM1-BP structures. However, semiempirical methods may underestimate the energetic impact of selective and strong protein−substrate interactions, which may be important in β-lactamase catalysis. To illustrate this point, we computed the energy of key interactions that are only present in the reactive TEM1-BP configurations (i.e., not in the prereactive complex) using the small model systems described in Figure S2 in the Supporting Information. These structures are meant to roughly estimate the interaction energy of Ser70 and Ser130 with the two Lys residues (73 and 234) within the active site at two stages along the reaction profile ($\mathbf{TS_1}$ and $\mathbf{TS_C}$ structures) and that of the forming ester with the "oxyanion hole" (**I** and $\mathbf{TS_2}$ structures). With respect to the correlated QM levels of theory (B3LYP/6-31+G* and MP2/6-31+G* including BSSE corrections[67]), we find that PM3 underestimates (by 3−7 kcal/mol) the interaction energies either for a $CH_3NH_3^+\cdots(CH_3O\cdot\cdot H-OCH_3)^-\cdots{}^+H_3NCH_3$ model or for an "oxyanion hole" model. Thus, these results suggest that our semiempirical calculations likely underestimate protein stabilization effects, which is not surprising given PM3's tendency to underestimate hydrogen bond strengths. Hence, we predict that the PM3 protein effects for the $\mathbf{TS_C}$, $\mathbf{TS_1}$, **I**, and $\mathbf{TS_2}$ TEM1-BP configurations are likely less than the true stabilization afforded by the protein. Furthermore, the impact of bulk solvent effects on the $\mathbf{TS_2}$ TEM1 BP structure (PM3 D&C−PB $\Delta\Delta G_{solvation} = +10.0$ kcal/mol) could be exaggerated by ∼4kcal/mol as suggested by the comparison between the B3LYP/6-31+G* and PM3 values for $\mathbf{TS_2}$ in Table 1. Finally, further catalytic advantage could come from entropic contributions arising from the structural elasticity[49] of the protein environment which are not considered in our model. Therefore, we conclude that, within the accuracy of our energy calculations, the hydroxyl and carboxylate-assisted pathway, cannot be ruled out.

Comparison with Experimental Kinetic Data. To find out if our results on the TEM1-BP models of the β-lactamase active site are realistic, we need to compare them with available experimental results. For example, it is clear that our TEM1-BP model is consistent with the most likely protonation state of the active-site residues. In addition, the hydroxyl and carboxylate-assisted process appears consistent with the complex pattern which emerges from mutagenesis experiments, especially those where the Lys73 and Lys234 residues were mutated.[17,19] Although these residues do not act as general bases in the catalytic mechanism, it has been suggested that their interactions with Ser70 and Ser130 may be an important electrostatic component of β-lactamase catalysis.[19] This correlates well with the anionic character of the Oγ@Ser70···H−Oγ@Ser130 contact at $\mathbf{TS_1}$ which can be particularly sensitive to the salt bridge interactions with either Lys73 or Lys234.

Of particular interest for further assessment of the viability of the hydroxyl and carboxylate-assisted mechanism are the β-secondary and solvent deuterium kinetic isotope effects[16] which represent properties of the transition state for the acylation of β-lactamases. As mentioned in the Introduction, the most direct conclusion from these studies is that no protons are "in flight" in the transition state, that is, protons are mere spectators to heavy atom rearrangement.[16] These results are surprising, however, in view of the many suggestions of general-base participation and the extended hydrogen-bond networks de-

scribed to deliver protons to the leaving amino group. Nonetheless, our theoretical characterization of significant configurations involved in the hydroxyl and carboxylate-assisted route, are nicely compatible with the kinetic isotope effects. For example, the two proton-transfer events in the hydroxyl and carboxylate assisted process, Ser70→carboxylate and carboxylate→ leaving N atom, take place with a low energetic cost at the initial and final stages of the acylation step, respectively. The high energy configurations in the middle of the reaction coordinate (**TS_1**, **I**, **TS_2**) are dominated by C−O bond formation and C−N bond breaking processes in agreement with the covalent chemistry assigned to the enzymatic rate-determining transition state.[16]

Effects of Ser130 Substitution. Another critical issue regarding the hydroxyl and carboxylate-assisted system is to determine whether our computationally derived model is compatible with the mutagenesis experiments of Ser130. The structural and functional roles of this residue have been studied via Ala, Asp, and Gly mutants.[17] These studies have highlighted the participation of Ser130 in the complex H-bond network in the active site and its potential role as a proton shuttle from the hydroxyl group of Ser70 to the leaving N atom. The different Ser130 mutants (specially the S130G mutant) can hydrolyze benzylpenicillin efficiently, with the observed differences in the k_{cat}/K_m values arising mainly from K_m. Previous molecular modeling studies[21] of the S130G mutant have shown that a water molecule can be placed at approximately the same position as that occupied by the Ser130 hydroxyl group in the wild type. All of these results suggest that a water molecule might play a similar catalytic role as a proton shuttle. To further clarify this point, we also located at the B3LYP/6-31+G* level the prereactive complex and the first TS structure corresponding to the water and carboxylate assisted methanolysis reaction of 3α-carboxypenam. The computed critical structures and their relative energies are shown in Figure S3 in the Supporting Information. We found that the geometry, charge distribution, transition vector and relative energies of the water-assisted TS were very similar to those of the methanol-assisted structure **TS_1** in Figure 2 (e.g., the energy barriers differed by less than 0.1 kcal/mol). Therefore, our theoretical calculations predict that replacement of the Ser130 side chain by a properly oriented water molecule bridging the Ser70 hydroxyl group and the β-lactam carboxylate, would lead to a catalytic mechanism basically identical to the hydroxyl and carboxylate-assisted route. Analogously, we also note that the hydroxyl and carboxylate-assisted mechanism would be essentially the same for class C β-lactamases in which the Ser130 residue is replaced by the Tyr150.

Role of the Carboxylate Group. In the TEM1-BP structures involved in the acylation step, the β-lactam carboxylate group does not have specific interactions with charged protein residues (i.e., the Arg244-carboxylate salt bridge is only present in the acylenzyme structure). This can facilitate the role of the penicillin carboxylate group in transferring a proton from Ser70 to the leaving N atom. The hydroxyl and carboxylate-assisted mechanism is also consistent with the experimental observation that esterification of the carboxylate group in penicillins decreases the enzyme rate enhancement by 10^4 in the class A β-lactamase from *Bacillus cereus*.[68] The fact that cephalosporins, whose carboxylate group has a different geometrical orientation to the β-lactam amide bond than do penicillins, are less susceptible to β-lactamase catalyzed hydrolysis, also supports an active kinetic role for the β-lactam carboxylate group in the enzymatic hydrolysis of penicillins. Nevertheless, it seems reasonable to expect that other proton-transfer pathways, not involving the β-lactam carboxylate group, may constitute competitive kinetic routes in the hydrolysis of other β-lactam substrates (e.g., cephalosporins) and/or in the mutants of the class A β-lactamases.

Summary

Our theoretical analyses of the reaction of benzylpenicillin catalyzed by the TEM1 protein indicates that the acylation of class A β-lactamases by penicillin proceeds through a hydroxyl and carboxylate-assisted mechanism. In this relatively simple mechanism, none of the catalytically important residues abstract a proton. Indeed, the hydroxyl group of Ser130 and the β-lactam carboxylate group define a favorable proton-transfer pathway from the Ser70 hydroxyl group to the leaving N atom. The ϵ-ammonium groups of Lys73 and Lys234 and the "oxyanion hole" formed by the backbone amide group of Ala237 and Ser70 play a central role in stabilizing the developing negative charge at the Oγ@Ser70 atom or at the β-lactam carbonyl oxygen along the reaction coordinate for acylation. In agreement with experimental kinetic isotope effects, the high-energy configurations of the hydroxyl and carboxylate-assisted mechanism involve uniquely covalent chemistry (formation of the C−O bond and cleavage of the C−N bond), whereas the proton-transfer events take place at the initial and final stages of the process. Moreover, the catalytic role of the Ser130 hydroxyl group can also be carried out by a water molecule.

Although more theoretical and experimental work will be necessary to definitively settle the nature of the mechanism of acylation of class A β-lactamases, the results of the present investigation on the hydroxyl and carboxylate-assisted pathway can help dispel the "enigmatic" nature of β-lactamase catalysis. Because the acylation machinery of the PBP enzymes,[69] class A β-lactamases, and class C β-lactamases turns out to be quite similar, we believe that the hydroxyl and carboxylate-assisted mechanism could be important for our understanding of the mode of action of the superfamily of active-site serine penicillin-recognizing enzymes.

Acknowledgment. We thank the NIH for support of this work via grant GM44974. We also thank the National Center for Supercomputer Applications (NCSA) for generous allocations of supercomputer time. N.D., D.S. and T.L.S. are grateful to MEC (Spain) for financial support (PB97-1300). N. D. also thanks MEC for Grant No. PB98-44430549.

Supporting Information Available: Table containing distances for the most important TEM1-BP contacts. Figure showing the model systems employed to estimate the strength of some key interactions in the TEM1 active site. Figure showing the prereactive complex and the first TS for the water and carboxylate-assisted methanolysis reaction of 3α-carboxypenam (3 pages). This material is available free of charge via the Internet at http://pubs.acs.org.

References and Notes

(1) Walsh, C. *Nature* **2000**, *406*, 775−781.
(2) Wright, G. D. *Chemistry & Biology* **2000**, *7*, 127−132.
(3) Maiti, S. N.; Philips, O. A.; Micetich, R. G.; Livermore, D. M. *Curr. Med. Chem.* **1998**, *5*, 441−456.
(4) Waley, S. G. *β-lactamase: Mechanism of Action* in *The Chemistry of β-Lactams*. Page, M. I., Ed.; Blackie Academic & Professional: London, 1992, pp 198−228.
(5) Pratt, R. F. *β-lactamase: Inhibition* in *The Chemistry of β-Lactams*; Page, M. I., Ed.; Blackie Academic & Professional: London, 1992, pp 229−271.
(6) Page, M. I. *J. Chem. Soc., Chem. Commun*. **1998**, 1609−1617.
(7) Wolfe, S. *Can. J. Chem*. **1994**, *72*, 1014−1032.

(8) Wang, Z.; Fast, W.; Valentine, A. M.; Benkovic, S. J. *Curr. Op. Chem. Biol.* **1999**, *3*, 614−622.
(9) Bush, K. *Clin. Infect. Dis*. **1998**, S48−53.
(10) Matagne, A.; Lamotte-Brasseur, J.; Frère, J. M. *Biochem. J.* **1998**, *330*, 581−598.
(11) Herzberg, O. *J. Mol. Biol.* **1991**, *217*, 701−719.
(12) Maveyraud, L.; Pratt, R. F.; Samama, J. P. *Biochemistry* **1998**, *37*, 2622−2628.
(13) Strydnadka, N. C. J.; Adachi, H.; Jensen, S. E.; Johns, K.; Sielecki, A.; Betzel, C.; Sutoh, K.; James, M. N. J. *Nature* **1992**, *359*, 700−705.
(14) Lobkovsky, E.; Moews, P. C.; Hansong, L.; Zhao, H. C.; Frére, J. M.; Knox, J. R. *Proc. Natl. Acad. Sci. U.S.A.* **1993**, *90*, 11 257−11 261.
(15) Christensen, H.; Martin, M. T.; Waley, S. G. *Biochem. J*. **1990**, *266*, 853−861.
(16) Adediran, S. A.; Deraniyagala, S. A.; Xu, Y.; Pratt, R. F. *Biochemistry* **1996**, *35*, 3604−3613.
(17) Matagne, A.; Frère, J. M. *Biochim. et Biophys. Acta* **1995**, *1246*, 109−127.
(18) Maveyraud, L.; Saves, I.; Burlet-Schitlz, O.; Swaren, P.; Masson, J. M.; Delaire, M.; Mourey, L.; Promé, J. C.; Samama, J. P. *J. Biol. Chem*. **1996**, *271*, 10 842−10 849.
(19) Lietz, E.; Truher, H.; Kahn, D.; Hokenson, M.; Fink, A. L. *Biochemistry* **2000**, *39*, 4971−4981.
(20) Lamotte-Brasseur, J.; Dive, G.; Dideberg, O.; Charlier, P.; Frére, J. M.; Ghuysen, J. M. *Biochem. J*. **1991**, *279*, 213−221.
(21) Lamotte-Brasseur, J.; Jacob-Dubuisson, F.; Dive, G.; Frère, J. M.; Ghuysen, J. M. *Biochem. J*. **1992**, *282*, 189−195.
(22) Vijayakumar, S.; Ravishanker, G.; Pratt, R. F.; Beveridge, D. L. *J. Am. Chem. Soc*. **1995**, *117*, 1722−1730.
(23) Ishiguro, M.; Imajo, S. *J. Med. Chem.* **1996**, *39*, 2207−2218.
(24) Gillaume, G.; Vanhove, M.; Lamotte-Brasseur, J.; Ledent, P.; Jamin, M.; Joris, B.; Frére, J. M. *J. Biol. Chem*. **1997**, *272*, 5438−5444.
(25) Dive, G.; Dehareng, D. *Int. J. Quantum Chem.* **1999**, *73*, 161−174.
(26) Wladowski, B. D.; Chenoweth, S. A.; Sanders, J. N.; Krauss, M.; Stevens, W. J. *J. Am. Chem. Soc.* **1997**, *119*, 6423−6431.
(27) Pitarch, J.; Pascual-Ahuir, J. L.; Silla, E.; Tuñón, I.; Moliner, V. *J. Chem. Soc., Perkin Trans. 2* **1999**, 1351−1356.
(28) Pitarch, J.; Pascual-Ahuir, J. L.; Silla, E.; Tuñón, I. *J. Chem. Soc., Perkin Trans. 2* **2000**, *4*, 761−767.
(29) a) Vilanova, B.; Donoso, J.; Frau, J.; Muñoz, F. *Helvetica Chim. Acta* **1999**, *82*, 1274−1288. (b) Frau, J.; Price, S. L. *Theor. Chim. Acta* **1997**, *95*, 151−163.
(30) Alvarez-Idaboy, J. A.; González-Jonte, R.; Hernández-Laguna, A.; Smeyers, Y. G. *J. Mol. Struct. (THEOCHEM)* **2000**, *504*, 13−28.
(31) Atanasov, B.; Mustafi, D.; Makinen, M. W. *Proc. Nat. Acad. Sci*. **2000**, *97*, 3160−3165.
(32) Ambler, R. P.; Coulson, A. F.; Frére, J. M.; Ghuysen, J. M.; Jaurin, B.; Joris, B.; Levesque, R.; Tiraby, G.; Waley, S. G. *Biochem. J*. **1991**, *276*, 269−272.
(33) Matagne, A.; Lamotte-Brasseur, J. Dive, G.; Knox, J. R.; Frère, J. M. *Biochem. J*. **1993**, *293*, 607−611.
(34) Raquet, X.; Lounnas, V.; Lamotte-Brasseur, J.; Frère, J. M.; Wade, R. C. *Biophys. J*. **1997**, *73*, 2416−2426.
(35) Lamotte-Brasseur, J.; Lounnas, V.; Raquet, X.; Wade, R. C. *Protein Sci*. **1999**, *8*, 408−409.
(36) Damblon, C.; Raquet, X.; Lian, L. Y.; Lamotte-Brasseur, J.; Fonzé, E.; Charlier, P.; Roberts, G. C. K.; Frére, J. M. *Proc. Natl. Acad. Sci. U.S.A.* **1996**, *93*, 1747−1752.
(37) Wolfe, S.; Kim, C. K.; Yang, K. *Can. J. Chem*. **1994**, *72*, 1033−1043.
(38) (a) Fersht, A. R.; Kirby, A. J. *J. Am. Chem. Soc.* **1967**, *89*, 4853−4856. (b) Fersht, A. R.; Kirby, A. J. *J. Am. Chem. Soc.* **1967**, *89*, 4857−4863.
(39) Díaz, N.; Suárez, D.; Sordo. T. L. *J. Am. Chem. Soc*. **2000**, *122*, 6710−6719.
(40) Gaussian 98, Revision A.6, Frisch, M. J.; Trucks, G. W.; Schlegel, H. B.; Scuseria, G. E.; Robb, M. A.; Cheeseman, J. R.; Zakrzewski, V. G.; Montgomery, J. A.; Stratmann, Jr., R. E.; Burant, J. C.; Dapprich, S.; Millam, J. M.; Daniels, A. D.; Kudin, K. N.; Strain, M. C.; Farkas, O.; Tomasi, J.; Barone, V.; Cossi, M.; Cammi, R.; Mennucci, B.; Pomelli, C.; Adamo, C.; Clifford, S.; Ochterski, J.; Petersson, G. A.; Ayala, P. Y.; Cui, Q.; Morokuma, K.; Malick, D. K.; Rabuck, A. D.; Raghavachari, K.; Foresman, J. B.; Cioslowski, J.; Ortiz, J. V.; Stefanov, B. B.; Liu, G.; Liashenko, A.; Piskorz, P.; Komaromi, I.; Gomperts, R.; Martin, R. L.; Fox, D. J.; Keith, T.; Al-Laham, M. A.; Peng, C. Y.; Nanayakkara, A.; Gonzalez, C.; Challacombe, M.; Gill, P. M. W.; Johnson, B.; Chen, W.; Wong, M. W.; Andres, J. L.; Gonzalez, C.; Head-Gordon, M.; Replogle, E. S.; Pople, J. A. Gaussian, Inc., Pittsburgh, PA, 1998.
(41) Hehre, W. J.; Radom, L.; Pople, J. A.; Schleyer, P. v. R. *Ab Initio Molecular Orbital Theory*; John Wiley & Sons Inc. New York, 1986.
(42) Becke, A. D. Exchange-Correlation Approximation in Density-Functional Theory In *Modern Electronic Structure Theory Part II*. Yarkony, D. R., Ed. World Scientific. 1995, Singapore.
(43) Curtiss, L. A.; Redfern, P. C. Smith, B. J.; Radom, L. *J. Chem. Phys*. **1996**, *104*, 5148−5152.
(44) Fukui, K. *Acc. Chem. Res.* **1981**, *14*, 363−368.
(45) Tomasi, J.; Persico, M. *Chem. Rev.* **1994**, *94*, 2027−2094.
(46) Tannor, D. J.; Barten, B.; Murphy, R.; Friesner, R. A.; Sitkoff, D.; Nicholls, A.; Ringnalda, M.; Goddard, W. A., III.; Honig, B. *J. Am. Chem. Soc.* **1994**, *116*, 11 875−11 882.
(47) JAGUAR 3.5, Schrödinger, Inc., Protland, OR, 1998.
(48) Reed, A. E.; Weinstock, R. B.; Weinhold, F. *J. Chem. Phys.* **1985**, *83*, 735−746.
(49) Taibi-Tronche, P. Massova, I.; Vakulenko, S. B.; Lerner, S. A.; Mobashery, S. *J. Am. Chem. Soc.* **1996**, *118*, 7441−7448.
(50) Jelsch, C.; Mourey, L.; Masson, J. M.; Samama, J. P. *Proteins: Struct. Func. Genet*. **1993**, *16*, 364−383.
(51) *LEaP*. Schafmeister, C.; Ross, W. S.; Romanovski, V. University of California San Francisco, 1995.
(52) Cornell, W. D.; Cieplak, P.; Bayly, C. I.; Gould, I. R.; Merz, K. M., Jr.; Ferguson, D. M.; Spellmeyer, D. C.; Fox, T.; Caldwell, J. W.; Kollman, P. A. *J. Am. Chem. Soc.* **1995**, *117*, 5179−5197.
(53) ROAR 2.0 Cheng, A.; Stanton, R. S.; Vincent, J. J.; van der Vaart, A.; Damodaran, K. V.; Dixon, S. L.; Hartsough, D.S.; Mori, M. Best, S. A.; Monard, G.; Garcia, M.; Van Zant, L. C.; Merz, K. M., Jr. **1999**, The Pennsylvania State University.
(54) Cheng, A.; Merz, K. M., Jr. *J. Phys. Chem.* **1996**, *100*, 1927−1937.
(55) Stewart, J. P. *J. Comput. Chem.* **1989**, *10*, 221−263.
(56) Field, M. J.; Bash, P. A.; Karplus, M. *J. Comput. Chem.* **1990**, *11*, 700−773.
(57) Monard, G.; Merz, K. M., Jr. *Acc. Chem. Res.* **1999**, *32*, 904−911.
(58) Liu, D. C.; Nocedal, J. *Math. Program*. **1989**, *45*, 503−528.
(59) Yang, W. T.; Lee, T. S. *J. Chem. Phys.* **1995**, *163*, 5674−5678.
(60) (a) Dixon, S. L.; Merz, K. M. Jr. *J. Chem. Phys.* **1996**, *104*, 6643−6649. (b) Dixon, S. L.; Merz, K. M., Jr. *J. Chem. Phys.* **1997**, *107*, 879−893.
(61) Gogonea, V.; Merz, K. M., Jr. *J. Phys. Chem. A.* **1999**, *103*, 5171−5188.
(62) DIVCON99: Dixon, S. L.; van der Vaart, A.; Gogonea, V.; Vincent, J. J.; Brothers, E. N.; Suárez, D.; Westerhoff, L. M.; Merz, K. M., Jr. **1999**, The Pennsylvania State University.
(63) van der Vaart, A.; Suárez, D.; Merz, K. M., Jr. *J. Chem. Phys.* **2000**, *113*, 10 512−10 523.
(64) Hokenson, M. J.; Cope, G. A.; Lewis, E. R.; Oberg, K. A.; Fink, A. L. *Biochemistry* **2000**, *39*, 6538−6545.
(65) Maveyraud, L.; Massova, I.; Birck, C.; Miyashita, K.; Samama, J. P.; Mobashery, S. *J. Am. Chem. Soc.* **1996**, *118*, 7435−7440.
(66) Bowden, K.; Bromley, K. *J. Chem. Soc., Perkin Trans 2*. **1990**, 2111−2116.
(67) van Duijneveldt, F. B.; van Duijneveldt-van de Rijdt, J. G. C. M.; van Lenthe, J. H. *Chem. Rev.* **1994**, *94*, 1873−1885.
(68) Laws, A. P.; Page, M. I. *J. Chem. Soc., Perkin. Trans. 2* **1989**, 1577−1581.
(69) Gordon, E.; Mouz, N.; Duée, E.; Dideberg, O. *J. Mol. Biol.* **2000**, *299*, 477−485.